NJC

Accepted Manuscript

This is an *Accepted Manuscript*, which has been through the Royal Society of Chemistry peer review process and has been accepted for publication.

Accepted Manuscripts are published online shortly after acceptance, before technical editing, formatting and proof reading. Using this free service, authors can make their results available to the community, in citable form, before we publish the edited article. We will replace this *Accepted Manuscript* with the edited and formatted *Advance Article* as soon as it is available.

You can find more information about *Accepted Manuscripts* in the Information for Authors.

Please note that technical editing may introduce minor changes to the text and/or graphics, which may alter content. The journal's standard Terms & Conditions and the Ethical guidelines still apply. In no event shall the Royal Society of Chemistry be held responsible for any errors or omissions in this *Accepted Manuscript* or any consequences arising from the use of any information it contains.

ROYAL SOCIETY OF CHEMISTRY

www.rsc.org/njc

Journal Name

RSCPublishing

ARTICLE

Rhodamine-based field-induced single molecule magnets in Yb(III) and Dy(III) series

Cite this: DOI: 10.1039/x0xx00000x

Wei Huang, Jun Xu, Dayu Wu,* Xingcai Huang and Jun Jiang

Received 00th January 2012,
Accepted 00th January 2012

DOI: 10.1039/x0xx00000x

www.rsc.org/

The reaction between rhodamine-6G-2-(hydrozinomethyl) quinolin-8-ol (**HQR1**) ligand and $Ln(tta)_3{\cdot}2H_2O$ precursors (tta = 2-thenoyltrifluoroacetone) leads to the formation of a series of mononuclear complexes with formula $[Ln(\mathbf{QR1})(tta)_2]{\cdot}(CH_3OH)_x(H_2O)_y$ (**3-6**) for (Ln=Yb, x=1, y=0 for **3**; Ln=Dy, x=1, y=0.5 for **4**; Ln=Tb, x=2,y=0 for **5**; Ln=Ho, x=2, y=0 for **6**) together with $[Dy(\mathbf{QR1})_2][NO_3]{\cdot}(CH_3OH)(H_2O)$ (**2**) and the reported $[Yb(\mathbf{QR1})_2][NO_3]{\cdot}(CH_3OH)(H_2O)_{0.5}$ (**1**), for the purpose of magnetic comparison. Their X-ray structures revealed that the coordination environment of each Ln(III) center is filled by two tta carboxylate groups and tetrachelate N_2O_2 binding site coming from the deprotonated **HQR1** ligand. The Yb and Dy complexes showed the field-induced slow relaxation of magnetization. Both Yb(III)-containing compounds were characterized by X-band EPR and magnetism studies, which revealed the different effective g values and slow paramagnetic relaxation. Comparison between two Yb(III) complexes **1** and **3** shows the magnetoanisotropy and barrier height of the magnetic relaxation are sensitive to the subtle change of the coordination environment of central metal ion. However, in Dy^{3+} series, QTM is difficult to overcome ever under *dc* field and the subtle variation of coordination environment leads to the tiny change in the energy barrier of slow magnetization relaxation. These results show that ligand-donating ability while maintaining molecular symmetry can be controlled to design single molecule magnets with enhanced relaxation barriers.

Introduction

Single-molecule magnets (SMMs) that exhibit slow relaxation of the magnetization below the blocking temperature (T_B) have attracted much interest due to the potential application in information storage,[1] quantum computing[2] and spintronics.[3] In the past 10 years, lanthanide single-molecule magnets (Ln-SMMs) have attracted much attention due to the fact that lanthanide ions possess significant single-ion magnetic anisotropy arising from the large unquenched orbital angular momentum and strong spin–orbit coupling.[4] High energy barriers (Δ/k_B) of representative Ln-SMMs were reported for the terbium(III) phthalocyaninato (Pc) double-decker compound,[5] dysprosium(III) *tert*-butoxide compound[6] and erbium(III) polyoxometallate sandwich compound[7] or erbium(III) organometallic sandwich compound.[8] Another important Kramers' ion Yb(III) with significant half-integer ground state should also lead to low-lying Kramers doublets with strong single-ion anisotropy.[9] However, because it is hard to pursue the proper ligands in the appropriate crystal field environment, there are less examples of Yb(III) SMMs than Dy(III) or Er(III)-based SMM.[10] The newly important work by O. Maury and coworkers successfully gave rise to a good correlation between magnetic and Yb(III) NIR-emissive properties.[11] Moreover, the near-infrared luminescent Yb(III) compounds are potential candidates for the light emitting diodes and bio-analysis and imaging,[12] which are the excellent materials for designing and envisaging the multifunctional luminescent SMMs.

Previously, we have demonstrated that the rhodamine-based ligand rhodamine-6G-2-(hydrozinomethyl) quinolin-8-ol (**HQR1**) is able to sensitise efficiently Yb(III) near-infrared luminescence and is key synthon to elaborate SMMs.[13] From the viewpoint of magnetochemistry, Long et al postulated that Yb(III) ion is predicted to have a prolate electron density when compared to Dy(III) ion.[9] Their hypothesis indicated that stronger equatorial coordination within a square antiprismatic coordination environment favours the well-separated $|M_J=\pm7/2>$ ground state, whereas stronger axial bond should stabilize $|M_J=\pm5/2>$ ground state. Significant separation between the ground state and the first excited state is a requisite for enhanced SMM behaviour.[14] Thus, from the combination between our previous structure observation of **$[Yb(QR1)_2][NO_3]$** and Long's recent hypothesis, it is attempted to employ a mixed ligand strategy where the presence of diketon-type coligand 2-thenoyltrifluoroacetone (abbreviated as **tta**) (Scheme 1) is ideal for coordination of metal ions as well as promoting the strength of Ln-donor interaction through

oxygen atom. The substituent strategy might contribute to the higher magnetic anisotropy and the enhanced reversal barrier of magnetization.[15] Interestingly, the dye-based Yb(III) and Dy(III) compounds can exhibit the slow relaxation of magnetization by taking advantage of unique ability of rhodamine derivative **HQR1** to act as rigid ligands offering a shielding environment. The comparison between compound 1 and 3 showed that the anisotropy can be tuned by the equatorial coordination to Yb(III) in our molecule toward the enhanced SMM behaviour.

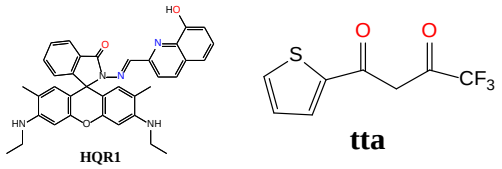

Scheme 1. Ligands HQR1 and tta Used in This Work

Experimental Section

General procedures and materials. All solvents were dried using standard procedures. $Ln(tta)_3{\cdot}2H_2O$ was prepared according to literature method.[16] All other reagents were purchased from Aldrich Co. Ltd and were used without further purification. The infrared (IR) spectra were recorded (400−4000 cm^{-1} region) on a Nicolet Impact 410 Fourier transform infrared spectrometer using KBr pellets. Elemental analyses (C, H, and N) were conducted with a Perkin-Elmer 2400 analyzer.

Fluorescent Measurements

Photo-induced emission spectra were undertaken on Edinburgh FS5 spectrometer. The absolute emission quantum efficiency was measured using the Edinburgh integrating sphere accessory following the De Mello method.[17]

Magnetic Measurements

Magnetic susceptibility measurements were performed using a Quantum Design MPMS XL-7 SQUID magnetometer. Diamagnetism was estimated from Pascal constants. The magnetic susceptibility measurements were taken between 2.0 and 300 K for dc-applied fields ranging from 0 to 70000 Oe. Direct-current (dc) susceptibility measurements were taken on a freshly filtered crystal sample wrapped in a polyethylene membrane. Complexes were prepared rapidly to avoid any loss of solvent. Alternating-current (ac) susceptibility measurements were taken using an oscillating ac field of 3 Oe and ac frequencies ranging from 1 to 1500 Hz under 0 and 1000 Oe applied static fields, respectively.

Synthetic Procedure

For the preparation of ligand **HQR1** and compound $\mathbf{[Yb(QR1)_2]NO_3{\cdot}(CH_3OH)(H_2O)_{0.5}}$ (**1**), see reference 13.

Preparation of compound $\mathbf{[Dy(QR1)_2][NO_3]{\cdot}(CH_3OH)(H_2O)}$ (**2**): An methanol solution(25ml) containing **HQR1**(0.1 mmol) was slowly added to methanol solution containing $Dy(NO_3)_3{\cdot}6H_2O$ (0.05 mmol). After stirring at reflux temperature for 30 min, the resulting solution was filtered and allowed to stand undisturbed in air. Dark-red block crystals were obtained by evaporating the concentrated solution at room temperature for several weeks. Yield: 38.3%. IR(KBr pallet cm^{-1}): 612.19(w), 673.28(w), 734.78(w), 845.97(w), 1018.66(w), 1113.15(w), 1191.35(w), 1313.54(m), 1386.04(s), 1447.13(w), 1497.23(s), 1530.62(m), 1564.02(w), 1608.82(s), 1653.22(w), 2359.54(w), 2914.62(w), 3418.82(s). Anal. Calcd for $Dy(C_{36}H_{33}N_5O_3)_2$ $(NO_3)(CH_3OH)(H_2O)$: H, 4.82; C, 61.22; N, 10.61. Found: H, 4.87; C, 60.58; N, 10.59.

Preparation of compound $\mathbf{[Yb(QR1)(tta)_2]{\cdot}(CH_3OH)}$ (**3**): An acetonitrile solution (10 mL) containing **HQR1** (0.1 mmol) was slowly added to a methanolic solution (10 mL) containing $Yb(tta)_3{\cdot}2H_2O$ (0.1 mmol). After stirring at room temperature for 15 min, the resulting solution was filtered and allowed to stand undisturbed in air. Dark-red block crystals suitable for X-ray diffraction were obtained by evaporating the concentrated solution at room temperature for several weeks. Yield: 54.8% (based on Yb). IR (KBr pallet, cm^{-1}): 580.72(w), 638.36(w), 683.36(w), 718.49(w), 747.49(w), 789.10(w), 837.06(w), 936.41(w), 1135.11(s), 1189.63(s), 1272.89(m), 1305.08(s), 1413.95(m), 1458.78(m), 1438.92(s), 1602.96(s), 2916.12(m), 3435.21(s). Anal. Calcd for $Yb(C_{36}H_{32}N_5O_3)$ $(C_8H_4SO_2F_3)_2(CH_3OH)$: H, 3.61 C, 51.75; N, 5.69. Found: H, 3.62; C, 51.72; N, 5.64.

Preparation of compound $\mathbf{[Dy(QR1)(tta)_2]{\cdot}(CH_3OH)(H_2O)_{0.5}}$ (**4**): The red block-shaped crystals of complex **4** suitable for X-ray diffraction were obtained in the similar manner to that described for complex **3** except that $Dy(tta)_3{\cdot}2H_2O$ was used instead of $Yb(tta)_3{\cdot}2H_2O$. Yield = 43.3%. IR (KBr pallet, cm^{-1}): 575.34(w), 642.12(w), 722.87(w), 742.21(w), 790.75(w), 835.43(w), 942.64(w), 1138.43(s), 1165.78(s), 1316.16(s), 1420.16(m), 1449.54(m), 1435.12(s), 1610.30(s), 2914.25(m), 3439.06(s). Anal. Calcd for $Dy(C_{36}H_{32}N_5O_3)(C_8H_4SO_2F_3)_2(CH_3OH)(H_2O)_{0.5}$: H, 3.72; C, 52.15; N, 5.74. Found: H, 3.78; C, 51.95; N, 5.79.

Preparation of compound $\mathbf{[Tb(QR1)(tta)_2]{\cdot}(CH_3OH)_2}$ (**5**): The dark-red well-shaped crystals of complex **5** suitable for X-ray diffraction were obtained by following the same procedure as that described for complex **3** except that $Tb(tta)_3{\cdot}2H_2O$ was used instead of $Yb(tta)_3{\cdot}2H_2O$. Yield = 65.3%. IR (KBr pallet, cm^{-1}): 586.12(w), 633.86(m), 685.96(w), 723.09(w), 753.12(w), 782.78(w), 935.03(w), 1138.65(s), 1191.56(s), 1245.12(m), 1321.82(s), 1421.06(m), 1454.54(m), 1441.67(s), 1621.50(s), 2911.78(m), 3439.75(s). Anal. Calcd for $Tb(C_{36}H_{32}N_5O_3)(C_8H_4SO_2F_3)_2(CH_3OH)_2$: H, 3.89; C, 51.97; N, 5.61. Found: H, 3.88; C, 51.64; N, 5.62.

Preparation of compound $\mathbf{[Ho(QR1)(tta)_2]{\cdot}(CH_3OH)_2}$ (**6**): The red pallet crystals of complex **6** suitable for X-ray diffraction were obtained by following the same procedure as that described for complex **3** except that $Ho(tta)_3{\cdot}2H_2O$ was used instead of $Yb(tta)_3{\cdot}2H_2O$. Yield = 75.2%. IR (KBr pallet, cm^{-1}): 568.87(w), 678.04(w), 740.89(w), 752.69(w), 788.90(w), 936.12(w), 1141.45(s), 1182.78(s), 1238.42(m), 1330.68(s), 1418.93(m), 1448.41(m), 1446.30(s), 1625.72(s), 2921.56(s), 3428.84(s). Anal. Calcd for $Ho(C_{36}H_{32}N_5O_3)(C_8H_4SO_2F_3)_2(CH_3OH)_2$: H, 3.86; C, 51.72; N, 5.58. Found: H, 3.87; C, 51.74; N, 5.53.

Table 1. Crystal Data and Structure Refinements for complexes **3**-**6**.

chemical formula	$C_{53}H_{44}YbF_6N_5O_8S_2$ (**3**)	$C_{53}H_{45}DyF_6N_5O_{8.50}S_2$ (**4**)	$C_{54}H_{48}F_6N_5O_9S_2Tb$ (**5**)	$C_{54}H_{48}F_6HoN_5O_9S_2$ (**6**)
formula mass	1230.09	1228.56	1248.01	1254.02
crystal system	triclinic	triclinic	triclinic	triclinic
space group	*P*-1	*P*-1	*P*-1	*P*-1
a (Å)	13.003(5)	13.001(3)	13.071(13)	13.023(4)
b (Å)	14.986(2)	14.987(17)	15.1300(7)	15.037(4)
c (Å)	15.684(2)	15.639(19)	15.7825(7)	15.687(4)
α(°)	117.719(4)	117.175(2)	118.258(3)	117.673(4)
β(°)	95.949(6)	95.878(3)	97.533(4)	96.460(2)
γ(°)	92.878(6)	92.955(3)	91.684(4)	92.480(2)
V (Å^3)	2674.0(11)	2680.0(8)	2710.6(3)	2687.3(13)
μ (mm^{-1})	1.905	1.551	1.462	1.631
Z	2	2	2	2
D_{calcd}(g/cm^3)	1.528	1.522	1.529	1.550
no. of reflections measured	15013	27811	20102	31111
no.of independent reflections	9311	9342	9458	9379
R_{int}	0.0775	0.0398	0.0515	0.0331
R_1[a]	0.0852	0.0493	0.0789	0.0394
wR_2[b] [I > 2σ(I)]	0.2059	0.1406	0.2025	0.1079
goodness of fit on F^2	1.071	1.086	1.019	1.090

[a]$R_1 = \Sigma(|F_o| - |F_c|)/\Sigma|F_o|$. [b]$wR_2 = \{\Sigma[w(F_o^2 - F_c^2)^2]/\Sigma[w(F_o^2)^2]\}^{1/2}$

X-ray Crystallography

The crystal data for all the complexes (Table 1) have been collected on a Bruker SMART CCD diffractometer (Mo Kα radiation, λ = 0.71073 Å).[18] SMART was used for collecting frames of data, indexing reflections, and determining lattice parameters, SAINT for integration of the intensity of reflections and scaling, SADABS for absorption correction, and SHELXTL for space group and structure determination and least-squares refinement on F^2.[19] All structures were determined by direct methods using SHELXS-97 and refined by full matrix least-squares methods against F^2 with SHELXL-97.[20] Hydrogen atoms were fixed at calculated positions, and their positions were refined by a riding model. All non-hydrogen atoms were refined with anisotropic displacement parameters. The crystallographic refinement was hindered due to the poor quality of **2** single crystal. CCDC 1400471 (**1**) and 1400472-1400475 (**3**-**6**) contain the crystallographic data.

Results and discussion

Structure Analysis

The structure of compound **[Yb(QR1)$_2$][NO$_3$]** · **(CH$_3$OH)(H$_2$O)$_{0.5}$** (**1**) was previously studied to discuss the dye-sensitized Yb(III) near-infrared emission. Bearing in mind that **tta** anion is a strong chelator to lanthanide ion, the compound **[Ln(QR1)(tta)$_2$]** · **(CH$_3$OH)$_x$(H$_2$O)$_y$** (Ln=Yb, *x*=1,*y*=0 for **3**; Ln=Dy, *x*=1, *y*=0.5 for **4**; Ln=Tb, *x*=2,*y*=0 for **5**; Ln=Ho, *x*=2, *y*=0 for **6**) were successfully isolated by the reaction of equimolar amounts of the tetrachelate ligand **HQR1**, **tta** ligand, and lanthanide 2-thenoyltrifluoroacetone. Suitable single crystals for X-ray diffraction analysis were obtained by the slow evaporation of the solution of these complexes in methanol/acetonitrile mixture. All compounds **3**−**6** are isostructural and crystallize in the triclinic space group *P*-1. As representative, the complex **3** was used for structural analysis. The asymmetric unit contains a single, complete mononuclear molecule. The Yb(III) ion is bound by two chelating **tta** ligands and one deprotonated **QR1** molecule, thus a triangular dodecahedron geometry (D_{2d}) is reserved according to SHAPE program.[21] (Fig. 1). The Ln−N bond length ranges from 2.427(10) to 2.562(10) Å, whereas the Ln−O bond length ranges from 2.234(11) to 2.409(9) Å for **3**. The displacement of one of **HQR1** ligands with two tta ligands decreases the corresponding Yb–donor bond distances by *ca.* 0.17 Å, which provide the stronger ligand field (LF). For the coordination environments of **1**-**6**, including distances of Ln-N and Ln-O and the angle around Ln(III) center, please turn to supporting materials, Table S3. The charge of Yb(III) is balanced by one deprotonated **QR1** and two tta anions, with solvent molecules of crystallization in the lattice. The monomers assemble together by pairs of face-to-face π…π interactions formed between the quinoline rings. The average separation found for this interaction for the compound is *ca.* 3.38 Å. (Figure S1, ESI).

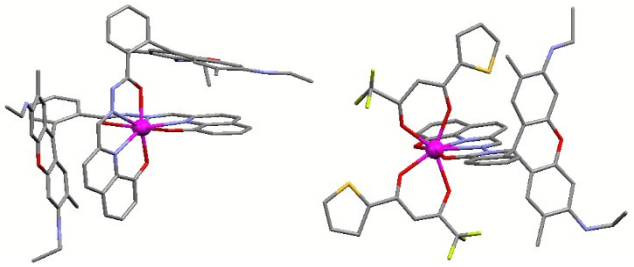

Fig. 1. X-ray structures of compound **1** and **3** with pink, gray, yellow, and red spheres representing Yb, C, S and O, respectively; hydrogen atoms and solvent molecules have been omitted for clarity.

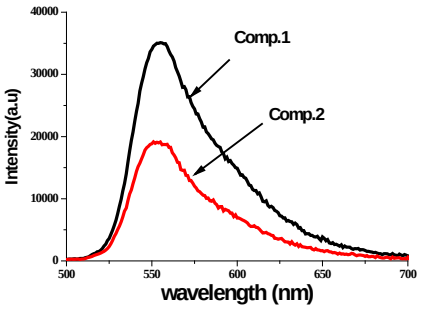

Fig. 2. Emission spectra of compound **1**-**2** with excitation at 480 nm (C = 5×10^{-6} M).

Table 2. Photophysical data of **1**-**2** in CH_3CN

Cpd	ε/M^{-1}cm^{-1}	λ_{em}[a]/nm	Φ[b] / %
Complex **1**	5710	552	51.14
Complex **2**	23270	555	21.97

Note: [a] excitation at 480 nm. [b] absolute quantum yield.

Fluorescent Property

The electronic absorption and fluorescence spectra of rhodamine lanthanide complexes **1**-**6** in acetonitrile solution are presented in Fig. **2** and S2, complexes **3**-**6** (5 μ mol L^{-1}) shows only a very weak absorption and emission (excitation at 480 nm), which is ascribed to its spirolactam form dominating in the solution as revealed in the X-ray diffraction structure. However, the characteristic absorption band appears in the range of 450–600 nm with a λ_{max} of 525 nm with ε = 5.71×10^3 and 2.33×10^4 L mol^{-1} cm^{-1} for complex **1** and **2**, respectively. In addition, a significant fluorescence corresponding to the delocalization in the xanthenes moiety of rhodamine was observed for **1** and **2** with quantum yield of 51.14% and 21.97%, respectively.[22] (Table 2)

Static Magnetic Property

The dc magnetic susceptibilities of **1** and **3** were measured from 300 to 2 K in applied magnetic fields (H) of 2500 Oe (Fig. 3a). At 300 K, the χ_MT value per Yb(III) ion is 2.22 cm^3 K mol^{-1} for **1** and 2.52 cm^3 K mol^{-1} for **3**, smaller than the value of 2.57 cm^3 K mol^{-1} expected for a Yb(III) ion ($^2F_{7/2}$, S = 1/2, L = 3, J = 7/2, g_J = 8/7),[23] which is ascribed to the incomplete pollution of the excited doublets due to the crystal-field effects. On lowering the temperature, χ_MT decreases continuously to 0.95 and 1.12 cm^3 mo1^{-1} K at 2 K for **1** and **3**, respectively. The downturn of each set of χ_MT value on cooling can be explained by depopulation of the Stark level split by the ligand field, suggesting the presence of significant magnetic anisotropy. On increasing the static field up to 70 kOe at 1.8 K, the magnetization for **1** and **3** reaches a value of 1.55 and 2.29 $N\beta$, respectively,(Fig. 3b) which is much lower than expected for free Yb(III) ions of ca. 4 $N\beta$, such behaviour can be attributed to the significant magnetic anisotropy for a lower effective spin.[24]

X-band ESR data, rarely reported for ytterbium(III) compounds, were collected on powder samples of **1** and **3** in order to evaluate electronic effective g-values.[25,26] The narrow parallel feature allows to discriminate the hyperfine pattern due to the active nuclei (^{171}Yb, I = 1/2, 14.28%).(Fig. 4) Thus, the effective g factors were obtained as following: g_{eff} = 5.35 for **1** and g_{eff} = 6.05 for **3**, respectively. Due to the smaller effective g value for **1**, at 1.8 K, the maximum in experimental Brillouin curve is obviously lower than that of **3** for an S_{eff} = 1/2 system, which is consistent with the EPR result.

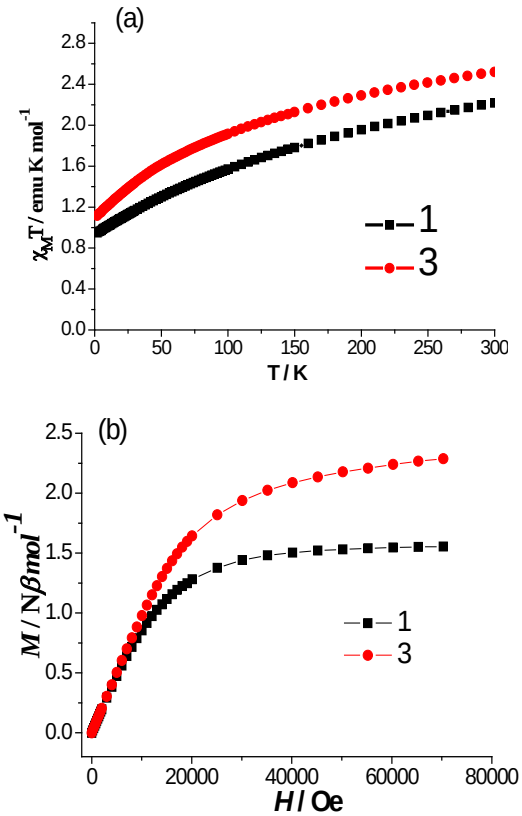

Fig. 3. (a) Temperature dependence of the χ_MT values for compounds **1** and **3** with an applied field of 2500 Oe. (b)Plots of magnetization upon the application of a magnetic field from 0 to 7 T at 1.8 K for compounds **1** and **3**.

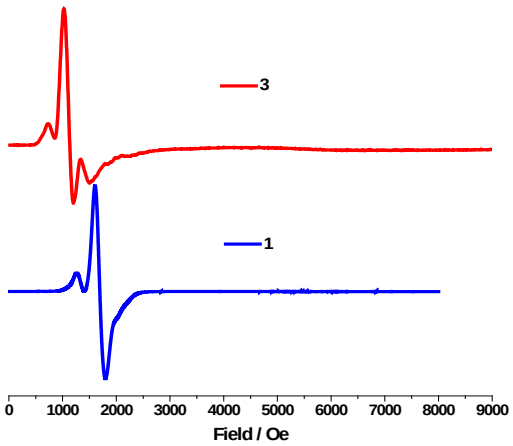

Fig. 4. X-band and EPR spectra of powder sample **1** and **3** collected at 5 K.

The direct current (dc) magnetic measurements were also performed on polycrystalline samples for the complexes **2**, **4-6** in the range of 2 to 300 K under an external field of 2500 Oe. At 300 K, the $\chi_M T$ values are 13.92, 14.02, 11.76, and 12.92 emu K mol^{-1} for **2**, **4**, **5**, and **6**, respectively. They are smaller than the expected paramagnetic values of 14.17, 11.82, and 14.07 cm^3 K mol^{-1} for Dy(III) ($^6H_{15/2}$, S = 5/2, L = 5, J = 15/2, g = 4/3), Tb(III) ($^7F_6$, S = 3, L = 3, J = 6, g = 3/2) and Ho(III) ($^5I_8$, S = 2, L = 6, J = 8, g = 5/4), respectively. (Fig. 5a). On cooling, $\chi_M T$ decreases rapidly below 50 K, which is most likely due to crystal-field effects (thermal depopulation of the M_J sublevels). The magnetizations of complexes 2, 4−6 from a zero dc field to 70 kOe at 1.8 K are shown in Fig. 5b. The magnetization increases rapidly at low field and then slowly reaches values of 6.74, and 7.62 $N\beta$mol^{-1} at 70 kOe for 5 and 6, respectively. The saturation value of complex **2** and **4** reaches 7.65 and 8.43 $N\beta$mol^{-1}. They are lower than the theoretical values of 9 $N\beta$mol^{-1} for Tb and 10 $N\beta$mol^{-1} for Dy and Ho, respectively, which can be attributed to the ligand-field-induced splitting of the Stark level as well as magnetic anisotropy with a lower effective spin.

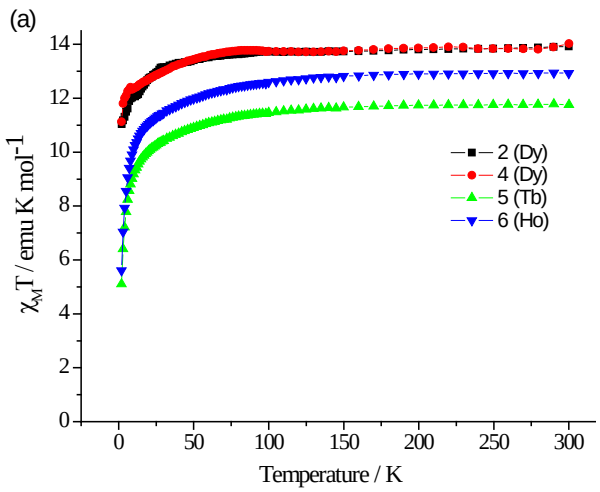

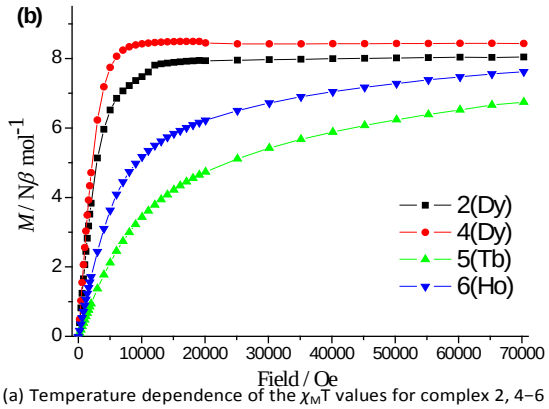

Fig. 5. (a) Temperature dependence of the $\chi_M T$ values for complex 2, 4−6 with an applied field of 2.5 kOe. (b) Plots of magnetization upon the application of a magnetic field from 0 to 7 T at 1.8 K for complex 2 and 4−6.

Dynamic Magnetic Properties of Yb(III) complexes 1 and 3

The EPR and *dc* magnetic analysis provided a sound description of the electronic structure of these systems, reflecting the character of magnetic anisotropy for two complexes on the basis of the prolate charge distribution of Yb(III) ion. Since **1** and **3** is characterized to be an almost easy-axis system, it may be expected to show slow relaxation of the magnetization at low temperature with an Arrhenius like dependence of the relaxation rate. Alternating current (*ac*) susceptibility measurements have been conducted on the compounds **1** and **3** to discuss the possibility of slow magnetic relaxation. At zero external field, no out-of-phase signal (χ'') for the ac susceptibilities are observed at frequencies of up to 1500 Hz and at temperatures down to 2 K for the compounds.(Figure. S3-4) This result indicates that the magnetization relaxation rate is very fast within the probed frequency.[27] Under an intermediate *dc* field (1 kOe), compounds **1** and **3** show obvious frequency dependence of both the in-phase (χ') and out-of-phase (χ'') susceptibility signals above 2 K, (Figure S5-6, Fig. 6), indicating the application of an external field shifts the characteristic maximum of χ'' to lower frequencies. The relaxation time is extracted from the fit of the frequency dependence of the ac susceptibility data between 2 and 6 K with an extended Debye model (Table S1 and Fig. 6). Below 3.5 K, the peaks of the χ'' signal for **1** can be found within frequency window of 1-1500 Hz, and the relaxation followed a thermally activated mechanism affording an energy barrier (Δ/k_B) of 5.37 K, with a pre-exponential factor τ_0 of 1.0×10^{-5} s based on the Arrhenius law [$\tau = \tau_0 \exp(\Delta/k_B T)$] (R = 0.9955) (Fig. 7). At fixed temperatures between 2 and 3.5 K, semicircle Cole-Cole plots (χ" vs. χ') were obtained and fitted by a generalized Debye model with the α parameter in the range 0.021–0.048(Fig. 8a, Table S1) indicating a narrow distribution of relaxation time (α = 0 for an ideal Debye model with a single relaxation time).[28]

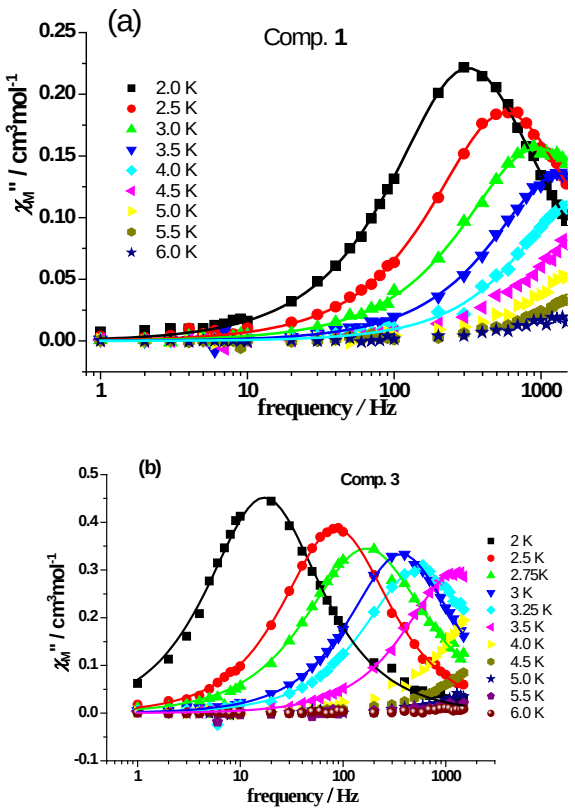

Fig. 6. Frequency dependence of the out-of-phase (χ″) signals for compound **1** and **3** from 2.0 to 6.0 K at a 1 kOe dc field. The solid lines represent the fit obtained with a generalized Debye model.

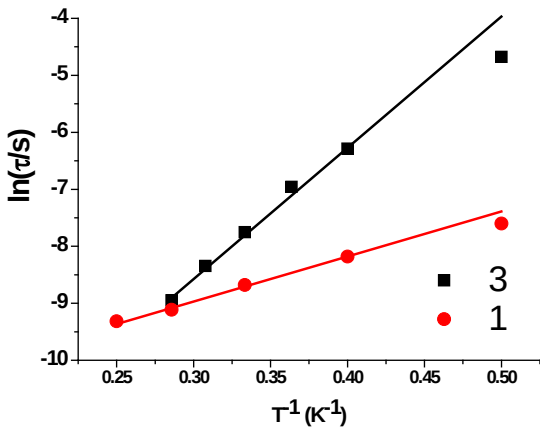

Fig.7. Arrhenius plot of the natural logarithm of relaxation time against reciprocal temperature for complexes **1** and **3**. Red and black lines are fits to the Arrhenius equation with parameters stated in the text.

For 3, the semicircular shapes of the Cole−Cole plots are also observed from 2.0 to 3.5 K (Fig. 8b), and the α parameter, fit to a generalized Debye model, is in the range of 0.02 to 0.09, also indicating that the relaxation followed a thermally activated mechanism with a single magnetic relaxation process dominant in this system. The Arrhenius law fit of the magnetization−relaxation parameter based on frequency-dependent ac susceptibilities afford an energy barrier (Δ/kB) of 16.1 K with a relaxation time (τ_0) of 1.78×10^{-7} s (R = 0.9901). (Fig. 7) The ac susceptibility confirms that the ground state is of Ising type with a relatively small barrier of 5.4 and 16.1 K for **1** and **3**, respectively, complex **3** is more anisotropic than complex **1**.[29,30]

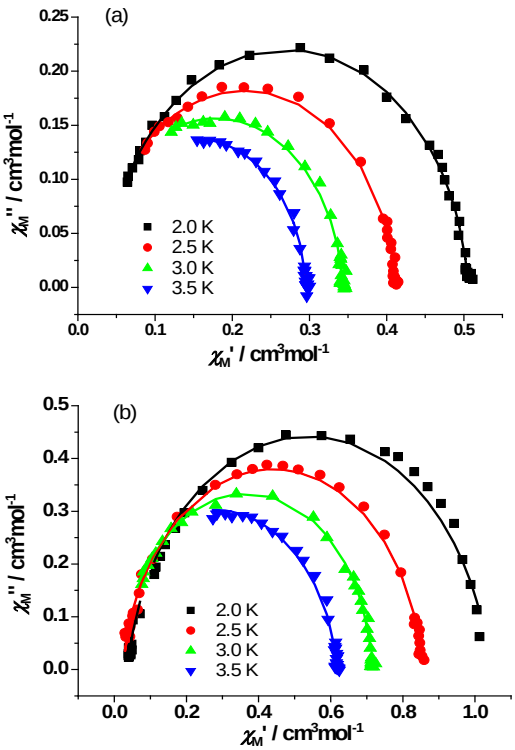

Fig.8. Cole−Cole plots for **1** (a) and **3** (b) obtained using the ac susceptibility data at a 1 kOe dc field. The solid lines correspond to the fit obtained to a general Debye model from 2.0 to 3.5 K.

Dynamic Magnetic Properties of Dy(III) complexes 2 and 4

In order to probe the possible slow relaxation of magnetization, the ac magnetic susceptibilities were conducted on **2**, **4**, **5** and **6** complexes under zero and none-zero field, respectively. Among the four investigated compounds, only compounds **2** and **4** show a significant out-of-phase component (χ_M'') in a nono-zero dc field (Fig. 9). The temperature dependence of the relaxation time at 1000 Oe extracted from the generalized Debye model at a given temperature is obtained through fitting the frequency dependent out-of-phase signals at different temperatures (Table S2). The relaxation time follows the Arrhenius law $\tau = \tau_0 \exp(\Delta/kT)$ only above 3 K with $\tau_0 = 4.3(6) \times 10^{-7}$ s and $\Delta = 20.0(6)$ K for **4** (R = 0.9920, Fig. 9c). Cole−Cole plots show semicircular shapes for temperatures higher than 3.0 K (Fig. S8). When the system enters the quantum regime at 2.0 K, the Cole−Cole plots become flattened and the fitting is of no sense. Higher temperatures and, thus, higher frequencies are required to reach a regime where only the thermal pathway is active in order to properly characterize the barrier height and characteristic time. However, the compounds **5** and **6** do not show a significant out-of-phase component (χ_M'') in a zero and nono-zero dc field, (see Fig.S9, S10) precluding the possibility of SMM behaviour.

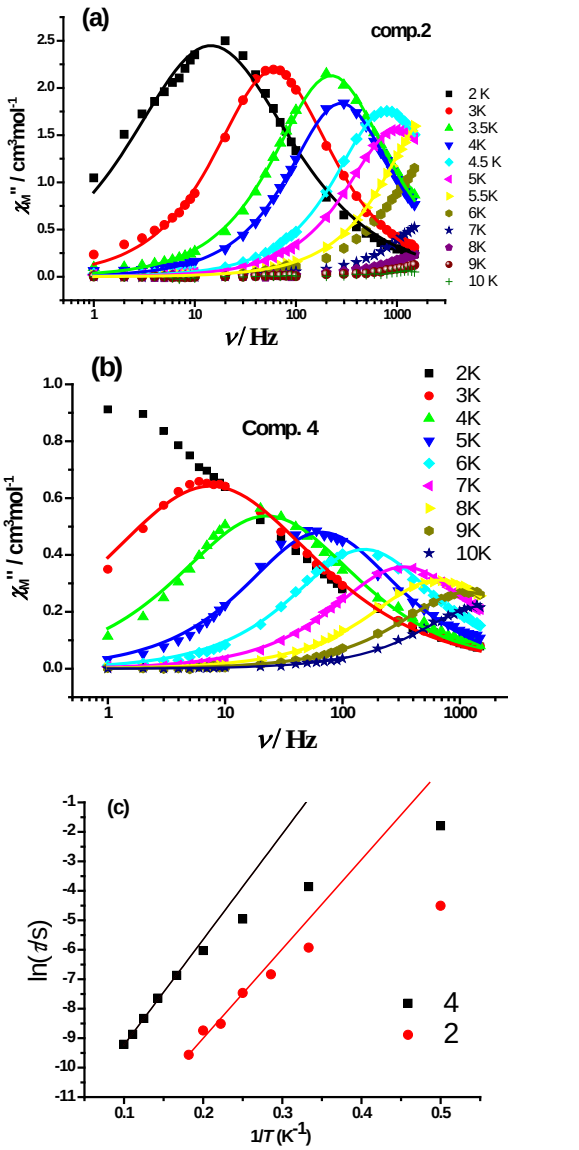

Fig. 9. Frequency dependence of out-of-phase (χ″) signals at different temperatures for **2** (a) and **4** (b) at 1 kOe. (c) Arrhenius plot of the natural logarithm of relaxation time against reciprocal temperature for complexes **2** and **4**.

However, for 2, the clear maximum peak of the χ″ signals can be found at temperatures higher than 3 K within the frequency window of 1-1500 Hz (Fig. 9a). The maximum peak of χ″ exhibits a significant shift toward the low-frequency region at a given temperature compared to compound 4, which allow one to accurately determine the energy barrier and characteristic time of relaxation. A corresponding Arrhenius law fit of the data gives an energy barrier of 24.8(4) K and a relaxation time $\tau_0 = 2.7(2) \times 10^{-6}$ s for **2** (R = 0.9987) (Fig. 9c). The large value of τ_0 indicates that even at high temperatures a pure thermal pathway is not realized and QTM is still active. Similar to that of complex **4**, this irregularity is also observed in the Cole−Cole plots at temperatures below 3 K (Figure S8, Supporting Information) because of the strong quantum tunneling effects in Dy(III)-based system.

It was reasoned that the differences in the magnetic relaxation observed between **1** and **3** were a consequence of contributions from the ligand donor atoms. Similar to that observed by Campbell, Mallah and co-workers,[31] where the small structural changes provoked by a slight alteration of the coordination environment lead to more anisotropic dysprosium(III) ion. In our case, the displacement of imine and quinoline N atoms with diketon O atoms would lead to the shorter Ln-donor bonds and a stronger over ligand field. As a result, the increased electron density results in a more anisotropic ground state for **3**, therefore, in a compound with a larger barrier of reorientation of the magnetization. Investigation of the dynamic magnetic properties of the oblate electron density distributions, such as Tb^{3+}, Dy^{3+} and Ho^{3+} metal ions, within the identical ligand field revealed the application of a small dc magnetic field lead to slow relaxation only for Dy^{3+}, in which QTM is difficult to overcome ever under *dc* field and the subtle variation of coordination environment leads to the tiny change in the energy barrier of slow magnetization relaxation.[32] On the other hand, the quantitative effects in height barriers, magnetization and *g*-values at low temperatures may be affected by dipolar interactions, which can be discarded by magnetic dilution.

Conclusions

In conclusion, we have prepared Yb(III) and Dy(III) rhodamine-based compounds through the ligand substituent that have different magnetic properties together with other lanthanide complexes including Tb(III) and Ho(III). Fluorescent experiment indicated the tta lanthanide series, **3-6**, are non-emissive, corresponding to the ring-closed spirolactam form as revealed in the X-ray diffraction structure. In contrast, lanthanide complexes **1** and **2** showed an intensive emission centered at 550 nm, characteristic of the ring-opened xanthenes moiety of rhodamine. Magnetic measurements revealed that the Dy(III) and Yb(III) complexes exhibit a field-induced slow relaxation of magnetization. The paramagnetic relaxation comparison between two Yb(III) compounds represents the quantitative comparison of the so-called single ion magnets (SIMs) with similar symmetry settings. The results confirm that the magnetic relaxation properties of Yb(III) complexes are very sensitive to tiny variations in the coordination configuration of the paramagnetic lanthanide ions. Although several groups attempted to theoretically calculate the *g*-factor anisotropy and the energy difference concerning the 1st excited state,[10c, d,f] to our best knowledge, ESR experimental evidence available to clarify this problem is still to be developed for Yb(III) system.[33] The study reported new type of lanthanide single-ion magnets with collective physical properties, i.e, near-IR luminescence for **1**,[13] as well as the magnetic slow relaxation. It will provide a starting point for further studies on dye-based mononuclear magnet, such as probing single-molecule behaviors by accurately placing them on surfaces to examine their magnetic properties.

Acknowledgements

The authors thank the anonymous referees' comments on the manuscript. We thank the financial support by the Priority Academic Program Development of Jiangsu Higher Education Institutions (PAPD). This experiment work is financially funded by NSFC program (21371010 & 21471023). We also thank SHMFF support of the low-temperature ESR measurement.

Notes and references

Jiangsu Key Laboratory of Advanced Catalytic Materials and Technology, School of Petrochemical Engineering, Changzhou University, Changzhou, Jiangsu 213164, China; E-mail: wudy@cczu.edu.cn

1. D. Gatteschi, A. Caneschi, L. Pardi and R. Sessoli, *Science*, 1994, **265**, 1054.
2. (a) M. N. Leuenberger and D. Loss, *Nature*, 2001, **410**, 789; (b) P. C. E. Stamp and A. Gaita-Arino, *J. Mater. Chem*., 2009, **19**, 1718.
3. (a) A. R. Rocha, V. M. García-suárez, S. W. Bailey, C. J. Lambert, J. Ferrer and S. Sanvito, *Nat. Mater.*, 2005, **4**, 335; (b) L. Bogani and W. Wernsdorfer, *Nat. Mater.*, 2008, **7**, 179; (c) M.Urdampilleta, S. Klyatskaya, J-P. Cleuziou, M. Ruben and W. Wernsdorfer, *Nat. Mater*., 2011, **10**, 502.
4. (a) C. Benelli and D. Gatteschi, *Chem. Rev.*, 2002**, 102**, 2369; (b) R. Sessoli and A. K. Powell, *Coord. Chem. Rev.*, 2009, **253**, 2328; (c)D. N. Woodruff, R. E. P. Winpenny and R. A. Layfield, *Chem. Rev.*, 2013, **113**, 5110; (d) F. Habib and M. Murugesu *Chem. Soc. Rev.*, 2013, **42**, 3278; (e) M. Sugita, N. Ishikawa, T. Ishikawa, S.Koshihara and Y. Kaizu, *Inorg. Chem*., 2006, **45**, 1299
5. (a) N. Ishikawa, M. Sugita, T. Ishikawa, S. Koshihara and Y. Kaizu,*J. Am. Chem. Soc.*, 2003, **125**, 8694; (b) C. R. Ganivet, B. Ballesteros, G. de la Torre, J. M. Clemente-Juan, E. Coronado and T.Torres, *Chem. –Eur. J*., 2013, **19**, 1457.
6. (a) A.-J. Hutchings, F. Habib, R. J. Holmberg, I. Korobkov, M. Murugesu, *Inorg. Chem.*; 2014, **53**, 2102. (b)R. J. Blagg, L. Ungur, F. Tuna, J. Speak, P. Comar, D. Collison, W.Wernsdorfer, E. J. L.McInnes, L. F. Chibotaru and R. E. P.Winpenny, *Nat. Chem*., 2013, **5**, 673.
7. M. A. AlDamen, J. M. Clemente-Juan, E. Coronado and C. Martí-Gastaldo and A. Gaita-Arinõ, *J. Am. Chem. Soc.*, 2008, **130**, 8874.
8. (a) S.-D. Jiang, B.-W. Wang, H.-L. Sun, Z.-M. Wang and S. Gao, *J.Am. Chem. Soc*., 2011, **133**, 4730; (b) K. R. Meihaus and J. R. Long,*J. Am. Chem. Soc.*, 2013, **135**, 17952; (c) L. Ungur, J. J. Le Roy, I. Korobkov, M. Murugesu and L. F. Chibotaru, *Angew. Chem. Int.Ed*., 2014, **53**, 4413.
9. J. D. Rinehart and J. R. Long, *Chem. Sci*., 2011, **2**, 2078.
10. (a)M. A. AlDamen, S. Cardona-Serra, J. M. Clemente-Juan, E. Coronado, A. Gaita-Arino, C. Marti-Gastaldo, F. Luis and O.95 Montero, *Inorg. Chem.*, 2009, **48**, 3467; (b) H. L. C. Feltham, F. Klower, S. A. Cameron, D. S. Larsen, Y. Lan, M. Tropiano, S.Faulkner, A. K. Powell and S. Brooker, *Dalton Trans.*, 2011, **40**,11425; (c) P.-H. Lin, W.-B. Sun, Y.-M. Tian, P.-F. Yan, L. Ungur,L. F. Chibotaru and M. Murugesu, *Dalton Trans*., 2012, **41**, 12349;100 (d) J.-L. Liu, K. Yuan, J.-D. Leng, L. Ungur, W. Wernsdorfer, F.-S.Guo, L. F. Chibotaru and M.-L. Tong, *Inorg. Chem*. 2012, **51**, 8538; (f) J. Ruiz, G. Lorusso, M.Evangelisti, E. K. Brechin, S. J. A. Pope and E. Colacio, *Inorg. Chem*. 2014, **53**, 3586.
11. (a) F. Pointillart, B. Le Guennic, S. Golhen, O. Cador, O. Maury and L.Ouahab. *Chem. Commun.*, 2013, **49**, 615; (b) G. Cosquer, F. Pointillart, J. Jung, B. Le Guennic, S. Golhen, O. Cador, Y. Guyot, A. Brenier, O. Maury and L. Ouahab. *Eur. J. Inorg. Chem.* 2014, **1**, 69.
12. (a) S. V. Eliseeva and J.-C. G. Bünzli, *Chem. Soc. Rev*., 2010, **39**,189; (b) J.-C. G. Bünzli, *Chem. Rev.*, 2010**, 110**, 2729.
13. W Huang, D.-Y. Wu, D. Guo, X. Zhu, C. He, Q. Meng and C.-Y. Duan. *Dalton Trans*., 2009, **2081,** 110.
14. K. R. Meihaus, S. G. Minasian, W. W. Lukens, Jr., S. A. Kozimor, D.K. Shuh, T. Tyliszczak and J. R. Long *J. Am. Chem. Soc.*, 2014, **136**,6056.14
15. (a) G. Cucinotta, M. Perfetti, J. Luzon, M. Etienne, P. E. Car, A. Caneschi, G. Calvez, K. Bernot and R. Sessoli, *Angew. Chem. Int.Ed.*, 2012, **51**, 1606; (b) J. B. José, C. S. Salvador, C. Eugenio, G. A. Alejandro, and P. Andrew, *Inorg. Chem*., 2012, **51**, 12565; (c) J. B. José, C. S. Salvador, C. Eugenio and P. Andrew, *J. Comput. Chem.*, **34**, 1961; (d) J. B. José, C. Eugenio and G. A. Alejandro, *Dalton Trans.*, 2012, **41**, 13705; (e) S. P. Kasper, U. Liviu, S. Marc, S. Alexander, S. M. Magnus, V. Veacheslav, M. Hannu, R. Stephane, W. Høgni, W. Oliver, F. C. Liviu, B. Jesper and J. Dreiser, *Chem. Sci.*, 2014, **5**, 1650.
16. A. I. Vooshin, N. M. Shavaleev and V. P. Kazakov, *J. Luminescence*, **2000**, *91*, 49.
17. J. C. de Mello, H. F. Wittmann and R. H. Friend, *Adv. Mater.* 1997, **9**, 230.
18. SMART & SAINT Software Reference Manuals, version 6.45; Bruker An alytical X-ray Systems, Inc.: Madison, WI, 2003.
19. G. M. Sheldrick, SADABS: Software for Empirical Absorption Correction, version 2.05; University of Göttingen: Göttingen, Germany, 2002.
20. G. M. Sheldrick, SHELXL97: Program for Crystal Structure Refinement; University of Göttingen: Göttingen, Germany, 1997.
21. M. Llunell, D. Casanova, J. Cirera, P. Alemany, S. Alvarez, Shape program, version 2, Universitat de Barcelona, Barcelona, Spain, 2010.
22. M. Beija, C.A.M. Afonso and J.M.G. Martinho, *Chem. Soc. Rev*., **2009**, *38*, 2410 and references therein.
23. O. Kahn, Molecular Magnetism; VCH: Weinhem, Germany, 1993.
24. F. Pointillart, B. Le Guennic, T. Cauchy, S. Golhen, O.Cador, O.Maury and L. Ouahab. *Inorg. Chem*. 2013, **52**, 5978.
25. A. Caneschi, A. Dei, D. Gatteschi, S. Poussereau and L. Sorace, *Dalton Trans*., 2004, 1048.
26. S. K. Langley, B. Moubaraki, C. M. Forsyth, I. A. Gass and K. S. Murray. *Dalton Trans*., 2010, **39**, 1705.120
27. F. Habib, J. Long, P.-H. Lin, I. Korobkov, L. Ungur, W. Wernsdorfer,L. F. Chibotaru and M. Murugesu, *Chem. Sci*. 2012, **3**, 2158.
28. K. S. Cole and R. H. Cole, *J. Chem. Phys.* 1941, **9**, 341.
29. K. R. Meihaus, S. G. Minasian, W.W. Lukens, Jr., S. A. Kozimor, D. K. Shuh, T. Tyliszczak and J. R. Long, *J. Am. Chem. Soc.*, 2014, **136**, 6056.
30. (a) J. Vallejo, I. Castro, R. Ruiz-García, J. Cano, M. Julve, F. Lloret, G. De Munno, W. Wernsdorfer and E. Pardo, *J. Am. Chem. Soc.* 2012, **134**, 15704. (b) X. Feng, J. Liu, T. D. Harris, S. Hill and J. R. Long, *J. Am. Chem. Soc*. 2012, **134**, 7521. (c) D. Wu, X. Zhang, P.

Huang, W.Huang, M. Ruan and Z. W. Ouyang, *Inorg. Chem.* 2013, **52**, 10976.

31. V. E. Campbell, H. Bolvin, E. Rivière, R. Guillot, W. Wernsdorfer and T. Mallah. *Inorg. Chem.*, 2014, **53**, 2598.

32. F. Aquilante, L. De Vico, N. Ferré, G. Ghigo, P.-Å. Malmqvist, P.Neogrády, T. B. Pedersen, M. Pitonak, M. Reiher, B. O. Roos, L. Serrano-Andrés, M. Urban, V. Veryazov and R. Lindh, *J. Comput. Chem*., 2010, **31**, 224.

33. For Dy(III) systems with EPR data, see: (a) U. J. Williams, B. D. Mahoney, P. T. DeGregorio, P. J. Carroll, E. Nakamaru-Ogiso, J. M. Kikkawa and E. J. Schelter, *Chem. Commun.* 2012, **48**, 5593-5595. (b) C.Ritchie, M.Speldrich, R. W. Gable, L. Sorace, P. Kögerler and C. Boskovic, *Inorg. Chem*. 2011, **50**, 7004–7014. (c) E. Lucaccini, L.Sorace, M. Perfetti, J.-P. Costes and R. Sessoli. *Chem. Commun.* 2014, **50**, 1648-1651.

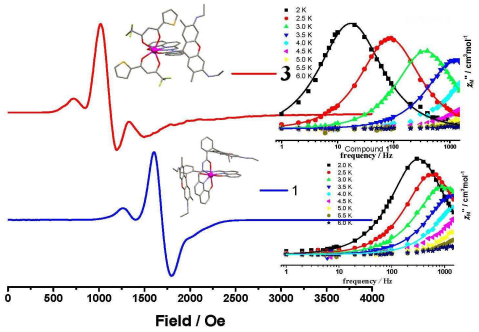

Dye-based rhodamine derivative has been utilized for the isolation of mononuclear lanthanide compounds characteristic of field-induced single molecule magnets.